Numerical Experiments on the Helmholtz Equation Derived From the Solar Radiation Transfer Equation in Three-Dimensional Space

Szu-Cheng S. Ou and Kuo-Nan Liou

Department of Meteorology
University of Utah
Salt Lake City, Utah 84112

Transmitted by A. Fymat

ABSTRACT

A numerical scheme using the finite-difference approach to solve the modified Helmholtz partial differential equation derived from the solar radiative transfer equation is developed and tested along with the method of evaluating the slant-path optical depth. For overhead solar incidence, we obtain good agreement between the finite-difference approach and the semianalytical solution in terms of the local intensity, local flux, average intensity, and average flux. For face-parallel oblique solar incidence in which the semianalytical method is not applicable, we compare the results with those of previous studies utilizing the Monte Carlo method and the approximate semianalytical method. We show that the present numerical scheme can be applied to any incident solar angle which the approximate semianalytical method is incapable of. Comparisons with results from Monte Carlo method reveal reasonable agreement for the averaged intensity and flux density.

1. INTRODUCTION

Theoretical study of the transfer of solar radiation in clouds usually has been carried out under the assumption that the atmosphere is plane-parallel. However, such an assumption is valid only when the horizontal extent of the scattering medium is much greater than the vertical dimension. It may be applicable to frontal or orographic clouds, which are normally stratified, but not to convective clouds, which are produced by thermal bubbles having large vertical extents. Clearly, a more appropriate assumption for the coordinate system is needed in order to investigate the processes of the transfer of solar radiation in finite cloud atmospheres by means of the basic radiative

0096-3003/80/060155+21$01.75

transfer equation. Coordinates such as Cartesian, cylindrical, or spherical may be utilized to describe the finite geometry of the cloud. Although these three-dimensional models would not fit the irregularly shaped finite clouds exactly, they would allow one to derive an approximate solution for the basic transfer equation and to obtain fundamental radiative parameters, which are essential to the interpretation of cloud sounding data from satellites and the evaluation of the global radiative heat budget involving cumulus-cloudy atmospheres.

Previous workers who have engaged in the study of the radiative transfer in finite clouds can be divided into two categories. The first group includes those who use the approximate semi-analytic method to solve the basic equation. Chandrasekhar [2], for example, has written down the fundamental transfer equation in Cartesian coordinates. Recently, Davies [3] solved the basic solar transfer equation for cuboidal clouds using the delta-Eddington approximation. Liou and Ou [4] investigated the transfer of infrared radiation in finite clouds based on the basic transport equation. The second group is those who use the Monte Carlo (MC) method to determine the average outward intensity and flux at the faces of clouds. McKee and Cox [5], for example, used the MC method to investigate the effect of the horizontal extent on the scattered radiation. Generally speaking, the MC method is quite accurate for the model assumed provided that sufficient photon histories are counted, but the computation time increases tremendously with increasing optical depths. On the other hand, the semianalytical method has been shown to be capable of producing reasonable flux data with relatively short computing time.

In this paper, we develop and test a numerical scheme using the finite-difference approach to solve the modified Helmholtz partial differential equation derived from the basic transfer equation in rectangular coordinates. The advantage of this scheme is that it can be applied to any incident solar angle. The approximate semianalytical method developed by Davies [3] and Liou and Ou [4], however, is incapable of solving the case involving arbitrarily oblique incident solar beam, owing to the complexity encountered in the direct solar attenuation term. We begin with the fundamental transfer theory and assume that clouds are homogeneous with respect to the single-scattering properties, i.e., the volume extinction cross-section, the single-scattering albedo, and the phase function. Analyses are carried out by expanding the phase function and intensity in normalized spherical harmonics in such a way that the basic transfer equation leads to a set of partial differential equations. The first approximation is then made, and it is shown that the problem reduces to solving the modified Helmholtz equation. Both the semianalytical and the numerical approaches are illustrated, along with the evaluation method of the slant path. To investigate the reliability of the

finite-difference numerical method, we first compare the resulting calculations from both approaches with respect to local and average intensity and flux density for the case of overhead solar incidence. We then compare the numerical solution with results from previous workers in terms of the average area-weighted intensity and flux density for the case of face-parallel oblique solar incidence.

2. BASIC EQUATIONS

The basic steady-state radiative transfer equation for homogeneous medium subject to a parallel incident light beam can be written as

$$\frac{1}{\sigma}(\Omega\cdot\nabla)I(\mathrm{s},\Omega)+I(\mathrm{s},\Omega)=\frac{\tilde{\omega}}{4\pi}\int_{4\pi}I(\mathrm{s},\Omega')P(\Omega,\Omega')\,d\Omega'$$

$$+\frac{\tilde{\omega}}{4\pi}P(\Omega,\Omega_0)\pi F\exp\left(-\int_s\sigma\,ds\right), \qquad (1)$$

where $I(\mathrm{s},\Omega)$ represents the monochromatic intensity in the direction Ω, σ the extinction coefficient, $\tilde{\omega}$ the single-scattering albedo, Ω' and Ω the unit vectors in incident and scattered directions, respectively, πF the incident solar flux in the direction Ω_0, and $P(\Omega,\Omega')$ the normalized scattering phase function. The scattering phase function for cloud particles in the solar spectrum is generally strongly peaked in the forward directions because of the strong diffraction peak. Finite expansion of the phase function in terms of known mathematical functions is inadequate, and significant errors may be produced in the transfer calculations. For this reason, it has been suggested that the phase function may be divided into two parts to better approximate the transfer calculations when finite terms are used for the phase-function expansion:

$$P(\Omega,\Omega')=4\pi f\delta(\Omega,\Omega')+(1-f)P', \qquad (2)$$

where f represents the fractional truncated forward peak, δ is the Kronecker delta function, and P' is a modified phase function. f can be determined either from a model phase function or from Mie scattering computations. It can be shown that a modified radiative transfer equation physically equivalent to Eq. (1) but consisting of parameters P', $\sigma'=\sigma(1-\tilde{\omega}f)$, and $\tilde{\omega}'=\tilde{\omega}(1-f)/(1-f\tilde{\omega})$ can be derived, allowing the incorporation of the diffraction peak of the phase function in the transfer analyses.

By expanding the modified phase function P' and the intensity I in terms of spherical harmonic functions $Y_l^m(\Omega)$ in a manner defined by Case and Zweifel [1], the modified radiative transfer equation can be decomposed into a series of partial differential equations upon making use of the orthogonality of the spherical harmonics [4]. If the expansions of both P' and I are truncated at the second term, i.e., $N=1$, where N is the maximum lower index in the truncated series, the following four partial differential equations may be derived:

$$\frac{\partial I_1^0}{\partial z}+\frac{1}{\sqrt{2}}\left(\frac{\partial}{\partial x}-i\frac{\partial}{\partial y}\right)I_1^{-1}-\frac{1}{\sqrt{2}}\left(\frac{\partial}{\partial x}+i\frac{\partial}{\partial y}\right)I_1^1 = -\sigma' I_0^0(1-\tilde{\omega}_0')+\frac{\tilde{\omega}'}{4}Fe^{-\tau_s'}, \quad (3)$$

$$\sigma'\left(1-\frac{\tilde{\omega}'g'}{3}\right)I_1^{-1}=-\frac{1}{3\sqrt{2}}\left(\frac{\partial}{\partial x}+i\frac{\partial}{\partial y}\right)I_0^0+\frac{1}{3\sqrt{2}}\frac{\tilde{\omega}'g'}{4}F(\Omega_{x,0}+i\Omega_{y,0})e^{-\tau_s'}, \quad (4)$$

$$\sigma'\left(1-\frac{\tilde{\omega}'g'}{3}\right)I_1^0=-\frac{1}{3}\frac{\partial I_0^0}{\partial z}+\frac{1}{3}\frac{\tilde{\omega}'g'}{4}F\Omega_{z,0}e^{-\tau_s'}, \quad (5)$$

$$\sigma'\left(1-\frac{\tilde{\omega}'g'}{3}\right)I_1^1=\frac{1}{3\sqrt{2}}\left(\frac{\partial}{\partial x}-i\frac{\partial}{\partial y}\right)I_0^0-\frac{1}{3\sqrt{2}}\frac{\tilde{\omega}'g'}{4}F(\Omega_{x,0}-i\Omega_{y,0})e^{-\tau_s'}, \quad (6)$$

where I_l^m is from the expansion

$$I(x,y,z;\Omega)=I_0^0(x,y,z)+\sqrt{3}\left[I_1^{-1}(x,y,z)Y_1^{-1}(\Omega)+I_1^0(x,y,z)Y_1^0(\Omega)+I_1^1(x,y,z)Y_1^1(\Omega)\right], \quad (7)$$

and $g'/3$ is the modified asymmetric factor obtained from the modified phase function. The quantity τ_s' is the optical depth in the direction of the incident beam. Thus, with the assumption of constant σ' we have

$$\tau_s'(\Omega_0)=\sigma' s(\Omega_0),$$

where $s(\Omega_0)$ is the distance between the point of interest in the medium and the point of entrance of the incident beam in the direction Ω_0. Upon substituting Eqs. (4)–(6) into Eq. (3), I_1^0, I_1^{-1}, and I_1^1 can be eliminated, and we obtain a modified Helmholtz equation in the form

$$\frac{\partial^2 I_0^0}{\partial x^2}+\frac{\partial^2 I_0^0}{\partial y^2}+\frac{\partial^2 I_0^0}{\partial z^2}-\lambda^2 I_0^0=-\xi e^{-\tau_s'}, \tag{8}$$

where

$$\xi=\left(1+\frac{g'}{3}-\frac{\tilde{\omega}'g'}{3}\right)\frac{3\tilde{\omega}'\sigma'^2}{4},$$

$$\lambda^2=3\sigma'^2(1-\tilde{\omega}')\left(1-\frac{\tilde{\omega}'g'}{3}\right).$$

In principle, Eq. (8) can be solved subject to proper boundary conditions and the function τ_s'. However, because of the directional dependence of τ_s', an analytical solution can be derived only for the sun overhead. For an oblique incident solar beam, the Helmholtz equation must be solved numerically.

To demonstrate the numerical approach we shall confine our study on the case of homogeneous cubic clouds. We may then define the unilateral optical depth, $\tau=\sigma a$, as a measure of the cloud dimension, with a being the geometrical length of any side of the cloud. In addition, we shall set the boundary conditions so that the incident flux densities on all faces of the cloud are zero. Upon defining a Cartesian coordinate system on the model cloud with the origin at one of the four corner points and letting the positive Z coordinate point downward, the flux density may be formulated as the hemispheric integral of the inner product of the intensity vector and the unit vector normal to the surface. Moreover, let $\pm x_i$ denote the direction of the positive or negative coordinate; we find

$$F_{\pm x_i}(x,y,z)=\int_{2\pi} I(x,y,z;\Omega)\Omega_{x_i}\,d\Omega, \tag{9}$$

where Ω_{x_i} is the directional cosine between the vector Ω and the coordinate $+x_i$. The value obtained from Eq. (9) can be positive or negative depending on the direction of F. A set of mixed boundary conditions can then be obtained by setting the incident flux at each face equal to zero. Upon

substituting Eqs. (4)–(7) into Eq. (9), we find

$$\left[\left(\frac{\partial I_0^0}{\partial x_i}\right) \pm h I_0^0\right]_{x_i=\left\{\begin{smallmatrix} a \\ 0 \end{smallmatrix}\right\}} = 3q\Omega_{x_i} e^{-\tau_s'}]_{x_i=\left\{\begin{smallmatrix} a \\ 0 \end{smallmatrix}\right\}}, \tag{10}$$

where $h=3\sigma'(1-\tilde{\omega}'g'/3)/2$, $q=\sigma'\tilde{\omega}'g'/12$, and x_i is either τ_x', τ_y', or τ_z'.

3. SEMIANALYTIC SOLUTION

For the case of overhead solar incidence where Ω_0 corresponds to the positive z-axis, i.e., $\Omega_x=\Omega_y=0$ and $\Omega_z=1$, Eq. (8) may be solved analytically, since the function τ_s' is simply equal to $\sigma' z$. Applying the method of separation of variables, the partial differential equation (8) with the imposed boundary conditions denoted in Eq. (10) may be solved by elementary methods and straightforward mathematical analyses. It can be shown that the solution for I_0^0 is given by

$$I_0^0(x,y,z)=\sum_{m=1}^{\infty}\sum_{n=1}^{\infty} W_{mn}(z)\cos(\lambda_m x')\cos(\lambda_n y'), \tag{11}$$

where

$$W_{mn}(z)=\frac{4\lambda_m\lambda_n}{[\lambda_m a+\sin(\lambda_m a)][\lambda_n a+\sin(\lambda_n a)]}$$

$$\times\left[A_{mn}e^{-\Lambda_{mn}(a-z)}+B_{mn}e^{-\Lambda_{mn}z}+\frac{C_{mn}\xi}{\Lambda_{mn}^2-\sigma'^2}e^{-\sigma' z}\right], \tag{12}$$

$$C_{mn}=\frac{4\sin(\lambda_m a/2)\sin(\lambda_n a/2)}{\lambda_m\lambda_n}, \tag{13}$$

$$x'=x-\frac{a}{2}, \tag{14a}$$

$$y'=y-\frac{a}{2}, \tag{14b}$$

$$\Lambda_{mn}^2=\lambda_m^2+\lambda_n^2+\lambda^2. \tag{15}$$

The eigenvalues λ_m and λ_n are the roots of the characteristic equation

$x = h\cot(xa/2)$, while the constants A_{mn} and B_{mn} are to be determined from the two boundary conditions at the surfaces $z=0$ and $z=a$. A Newton's iteration method was employed to determine the eigenvalues λ_m and λ_n.

4. FINITE-DIFFERENCE SCHEME

a. Evaluation of $\tau_s'(x,y,z)$

For an oblique solar incidence angle, evaluation of the optical depth for a given locality in the cloud $\tau_s'(x,y,z)$ in the direction of Ω_0 requires information on the geometry of the model cloud and the three direction cosines $\Omega_{x,0}$, $\Omega_{y,0}$, and $\Omega_{z,0}$ of the unit vector Ω_0. As shown in Fig. 1, a light beam which is obliquely incident at the origin of the rectangular coordinates forms three planes with respect to the $x, y,$ and z axes. These planes subdivide the entire cube into three zones. The scattering medium in zones 1, 2, and 3 is subject to the directly transmitted sunlight, which is incident on the three sunlit surfaces represented by $y=0$, $x=0$, and $z=0$, respectively. It follows that the dividing planes can be represented by three equations in terms of $\Omega_{x,0}$, $\Omega_{y,0}$, and $\Omega_{z,0}$ in the forms

$$y = \frac{\Omega_{y,0}}{\Omega_{z,0}} z, \tag{16a}$$

$$x = \frac{\Omega_{x,0}}{\Omega_{z,0}} z, \tag{16b}$$

$$y = \frac{\Omega_{y,0}}{\Omega_{x,0}} x. \tag{16c}$$

To evaluate $\tau_s'(x,y,z)$, we need to specify the locality of (x,y,z) with reference to one of the three zones. Based on Eqs. (16a) and (16c), if $y < (\Omega_{y,0}/\Omega_{z,0})z$ and $y < (\Omega_{y,0}/\Omega_{x,0})x$, then the point (x,y,z) is to be considered in zone 1. Likewise, from Eqs. (16b) and (16c), if $x < (\Omega_{x,0}/\Omega_{z,0})z$ and $y < (\Omega_{y,0}/\Omega_{x,0})x$, the point (x,y,z) is in zone 2. If neither of the above tests is met, the point (x,y,z) must lie in zone 3. Once a specific point (x,y,z) has been assigned to a zone, the function τ_s' can be evaluated as follows:

$$\tau_s'(x,y,z;\Omega) = \sigma' y/\Omega_{y,0} \qquad \text{for zone 1,} \tag{17a}$$

$$\tau_s'(x,y,z;\Omega) = \sigma' x/\Omega_{x,0} \qquad \text{for zone 2,} \tag{17b}$$

$$\tau_s'(x,y,z;\Omega) = \sigma' z/\Omega_{z,0} \qquad \text{for zone 3.} \tag{17c}$$

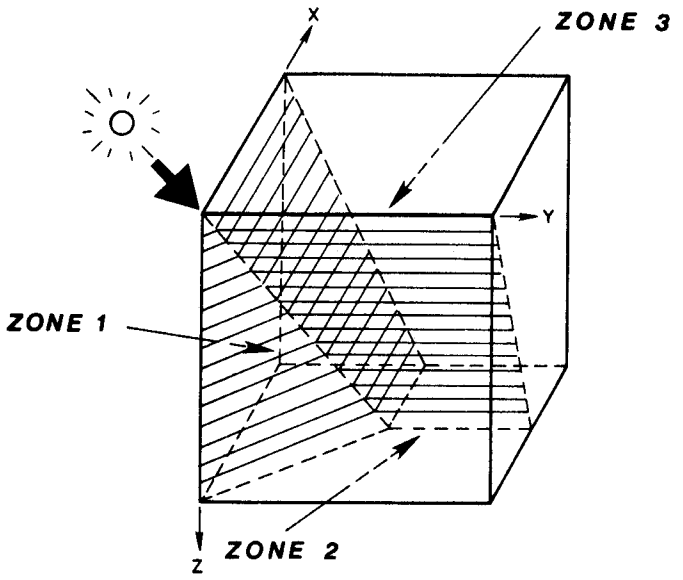

FIG. 1. The decomposition of the model cubic cloud into three zones based on the directional cosines of the incident solar beam with respect to the coordinate axes.

It should be noted that for the special case where the incident beam is parallel to a pair of opposite surfaces (for example, the surfaces corresponding to $y=0$ and $y=a$), there are only two zones involved, namely, zone 2 and zone 3. Under this situation, evaluation of τ_s' requires only Eqs. (17b) and (17c).

b. Numerical Algorithm

We employ a finite-difference scheme to solve the partial differential equation and the boundary conditions denoted in Eqs. (8) and (10), respectively. For simplicity, let the solution be denoted by $U(x,y,z)$, which is equivalent to $I_0^0(x,y,z)$. We first divide the model cube into N^3 cubic cells with $(N+1)^3$ grid points and uniform increment length, d. We then label each grid point with a set of indices (i,j,k) such that $x(i)=(i-1)d$, $Y(j)=(j-1)d$ and $z(k)=(k-1)d$. By using the three-point form as an approximation to the second-order partial differential equation, Eq. (8) may be replaced by the following finite difference form (see, e.g., [6]):

$$U_{i+1,j,k}+U_{i-1,j,k}+U_{i,j+1,k}+U_{i,j-1,k}+U_{i,j,k+1}+U_{i,j,k-1}-(6+d^2\lambda^2)U_{i,j,k}=-\xi e^{-\tau_s'(i,j,k)}. \quad (18)$$

Similarly, upon replacing the first-order partial differentials given in Eq. (10) by a five-point approximation form, we have for any coordinate x_i,

$$\sum_{l=0}^{4} a_l U\Big|_{x_i=ld} = 3q\Omega_{x_i} e^{-\tau_i'}\Big]_{x_i=0}, \tag{19a}$$

$$\sum_{l=0}^{4} a_l U\Big|_{x_i=(N-l)d} = -3q\Omega_{x_i} e^{-\tau_i'}\Big]_{x_i=a}, \tag{19b}$$

where the a_l's can be determined from Taylor's theorem as follows: $a_0 = hd + \frac{25}{12}$, $a_1 = -4$, $a_2 = 3, a_3 = -\frac{4}{3}$, and $a_4 = \frac{1}{4}$. Equations (18) and (19) give a total number of $(N-1)^3 + 6(N+1)^2$ linear equations. However, there are only $(N+1)^3$ unknowns, and so the number of equations is more than that of unknowns by $4N^2 + 12$. This can be attributed to the discontinuity manifested at the corner points, i.e., the intersection of either two or three neighboring surfaces. For example, the value of $U_{1,1,k}$ at the intersection of the planes $x=0$ and $y=0$ obtained from Eq. (19a) with x_i corresponding to the x-axis may differ from that obtained from the same equation with x_i corresponding to the y-axis, so that two different quantities for $U_{1,1,k}$ might be resulted. Theoretically, if the incremental length d is made infinitesimally small, the difference should reduce to zero. The same argument can be applied to the intersection of three neighboring surfaces. In real calculation, however, as the quantity d can not be made zero, we average the values obtained from Eq. (19a) with different coordinates x_i for the corner points. To perform the averaging, $U_{i,j,k}$ at points other than corner points must be first obtained. The Gauss-Seidel iteration method is utilized to compute $U_{i,j,k}$ at these points.

5. DEFINITION OF RADIATION PARAMETERS

Once the point values of I_0^0 (or U) have been determined, we may then proceed to compute the local and average intensity and flux density.

a. Local Intensity

The expressions for the local intensity can be obtained by substituting Eqs. (4)–(6) into Eq. (7). Thus, letting x_i be the x-, y-, or z-axis, we find

$$I(x,y,z;\Omega) = I_0^0(x,y,z) - \frac{3}{2h}\sum_{i=1}^{3} \frac{\partial I_0^0(x,y,z)}{\partial x_i}\Omega_{x_i} + \frac{9q}{2h}(\Omega\cdot\Omega_0)e^{-\tau_i'} \quad . \tag{20}$$

The intensity on the surface of the cloud can be further simplified by inserting the boundary conditions represented by Eq. (10). The difference in the determination of the point intensity between the semianalytical method and the numerical method for the overhead incidence case is caused by the computation of the partial differential terms $-\partial I_0^0/\partial x_i$ and the quantity I_0^0. In the former case, I_0^0 is obtained from Eq. (11), and one then differentiates the same equation with respect to the coordinate x_i to derive $-\partial I_0^0/\partial x_i$. In the latter case, U, which is the approximate value of I_0^0, is obtained by means of the procedure outlined in Sec. 4, and the partial differential terms are determined by the two-point form (Euler's rule) for interior points, and by Eq. (10) for the boundary points.

b. Local Flux Density

The flux density at any point in the direction of either the $+x_i$-axis or the $-x_i$-axis can be derived from Eqs. (7) and (9) in the form

$$F_{\pm x_i}(x,y,z)=\pi\left[I_0^0(x,y,z)\mp\frac{1}{h}\frac{\partial I_0^0(x,y,z)}{\partial x_i}\pm\frac{3q}{h}\Omega_{x_i}e^{-\tau/}\right]. \tag{21}$$

Since at each cloud surface, the incoming flux density is assumed to be zero, the outgoing flux density in the direction normal to the surface becomes $2\pi I_0^0$ regardless of the surfaces.

c. Average Intensity

Averaging over the point intensity may be carried out either with respect to a single face of the cube or with respect to two or three faces. For the case of overhead sun, the average intensity for a single face may be derived simply by integrating the intensity expression given by Eq. (20) over the appropriate area. We obtain the following forms for the single-face average intensity:

$$\bar{I}(\Omega)\big]_{z=0}=\frac{1}{a^2}\left(1-\tfrac{3}{2}\Omega_z\right)\sum_m\sum_n W_{mn}(z=0)C_{mn}, \tag{22a}$$

$$\bar{I}(\Omega)\big]_{z=a}=\frac{1}{a^2}\left(1+\tfrac{3}{2}\Omega_z\right)\sum_m\sum_n W_{mn}(z=a)C_{mn}, \tag{22b}$$

$$\bar{I}(\Omega)\big]_{x=0}=\frac{1}{a^2}\sum_m\sum_n\left[\left(1-\tfrac{3}{2}\Omega_x\right)\tilde{W}_{mn}C_{mn}\frac{\lambda_m^2}{2h}+\tilde{W}'_{mn}C_{mn}\Omega_z\frac{3\lambda_m^2}{4h^2}+\frac{9qa\sigma'}{2h}\left(1-e^{-\sigma' a}\right)\right], \tag{22c}$$

where

$$\tilde{W}_{mn} = \int_0^a W_{mn}(z)\,dz,$$

$$\tilde{W}'_{mn} = -\int_0^a \frac{dW_{mn}(z)}{dz}\,dz.$$

The remaining single-face average intensities, $\bar{I}(\Omega)|_{x=a}$, $\bar{I}(\Omega)|_{y=0}$, and $\bar{I}(\Omega)|_{y=a}$, can be obtained from Eq. (22c) by using the symmetry of the side faces. If we now define an emergent direction vector Ω_e in terms of the zenith angle θ with respect to the outward surface normal and the azimuthal angle ϕ with respect to the $-z$-axis for the four side surfaces, it is seen that $\bar{I}(\Omega_e)|_{x=0} = \bar{I}(\Omega_e)|_{x=a} = \bar{I}(\Omega_e)|_{y=0} = \bar{I}(\Omega_e)|_{y=a}$. However, this equality is only applicable to the overhead incidence case.

The numerical method for computing $\bar{I}(\Omega)$ for both overhead and oblique solar incidence employs the two-dimensional trapezoidal rule to evaluate the surface integral involved. It turns out that there is no need to evaluate the partial differential terms involved in Eq. (20), but rather we may utilize the known values of I_0^0, i.e., U in the numerical computations. As an illustrative example, the expression for $\bar{I}(z=0;\Omega)$ is given by

$$\begin{aligned}
\bar{I}(z=0;\Omega) = {} & \frac{d^2}{(\sigma' a)^2} \\
& \times \Bigg\{ \left(1-\tfrac{3}{2}\Omega_z\right) \sum_{i=1}^{N} \sum_{j=1}^{N} \tfrac{1}{4}\left(U_{i,j,1} + U_{i+1,j,1} + U_{i,j+1,1} + U_{i+1,j+1,1}\right) \\
& + \frac{3}{2hd}\Omega_x \sum_{j=1}^{N} \tfrac{1}{2}\left[\left(U_{1,j,1} + U_{1,j+1,1}\right) - \left(U_{N,j,1} + U_{N,j+1,1}\right)\right] \\
& + \frac{3}{2hd}\Omega_y \sum_{i=1}^{N} \tfrac{1}{2}\left[\left(U_{i,1,1} + U_{i+1,1,1}\right) - \left(U_{i,N,1} + U_{i+1,N,1}\right)\right] \\
& + \frac{9q}{2h}\left(\Omega_x \Omega_{x,0} + \Omega_y \Omega_{y,0}\right) \sum_{i=1}^{N} \sum_{j=1}^{N} \tfrac{1}{4}\left[e^{-\tau'_s(i,j,1)} + e^{-\tau'_s(i+1,j,1)}\right. \\
& \left. + e^{-\tau'_s(i,j+1,1)} + e^{-\tau'_s(i+1,j+1,1)}\right] \Bigg\}. \qquad (23)
\end{aligned}$$

The average intensities over other faces may be evaluated in a manner similar to the above equation.

From the spacecraft point of view, the observed intensity at an oblique angle with respect to the cubic cloud includes the contributions from the top as well as from the side surfaces. Thus, we define a parameter referred to as the area-weighted intensity as detected by the scanning instrument in the form

$$\bar{I}_{aw}(\Omega)=\frac{\bar{I}(z=0;\Omega)|\Omega_z|+\bar{I}(x=0 \text{ or } a;\Omega)|\Omega_x|+\bar{I}(y=0 \text{ or } a;\Omega)|\Omega_y|}{|\Omega_x|+|\Omega_y|+|\Omega_z|}. \quad (24)$$

It follows that the computed area-weighted intensity may be used for comparison with the observed intensity reflected by a finite cloud.

d. Average Flux Density

Since the outward flux density at all surfaces is equal to $2\pi I_0^0$, the average outward flux density is simply the average of I_0^0 multiplied by 2π. Semianalytically (for overhead incidence), we integrate Eq. (11) analytically to obtain an expression in series expansions. Thus, we find

$$\bar{F}_{-z}(z=0)=\frac{2\pi}{a^2}\sum_m\sum_n W_{mn}(z=0)C_{mn}, \quad (25a)$$

$$\bar{F}_{+z}(z=a)=\frac{2\pi}{a^2}\sum_m\sum_n W_{mn}(z=a)C_{mn}, \quad (25b)$$

$$\bar{F}_{-x}(x=0)=\frac{2\pi}{a^2}\sum_m\sum_n \tilde{W}_{mn}C_{mn}\frac{\lambda_m^2}{2h}. \quad (25c)$$

Again $\bar{F}_{-x}(x=0)$, $\bar{F}_{+x}(x=a)$, $\bar{F}_{-y}(y=0)$, and $\bar{F}_{+y}(y=a)$ are all identical. The numerical approach, on the other hand, employs the two-dimensional trapezoidal rule to integrate I_0^0 over the surface. Thus, we have

$$\bar{F}_{-z}(z=0)=\frac{2\pi}{a^2}\sum_{i=1}^{N}\sum_{j=1}^{N}\frac{d^2}{4}(U_{i,j,1}+U_{i+1,j,1}+U_{i,j+1,1}+U_{i+1,j+1,1}), \quad (26a)$$

$$\bar{F}_{+z}(z=a)=\frac{2\pi}{a^2}\sum_{i=1}^{N}\sum_{j=1}^{N}\frac{d^2}{4}(U_{i,j,N+1}+U_{i+1,j,N+1}+U_{i,j+1,N+1}+U_{i+1,j+1,N+1}), \quad (26b)$$

$$\bar{F}_{-x}(x=0)=\frac{2\pi}{a^2}\sum_{i=1}^{N}\sum_{j=1}^{N}\frac{d^2}{4}(U_{1,i,j}+U_{1,i+1,j}+U_{1,i,j+1}+U_{1,i+1,j+1}), \quad (26c)$$

where all the symbols have been defined previously.

6. RESULTS AND DISCUSSION

a. Overhead Solar Incidence

We first compare the resulting computations using the semianalytical method and the numerical finite-difference method to examine the relative accuracy of the latter approach. In the numerical experiments the single-scattering albedos used were 0.9 and 1, the incident solar flux was assumed to be unity, the range of the optical depth was from 0.5 to 50, and the asymmetry factor and the fraction of the diffraction peak were 0.75 and 0.625, respectively.

In Fig. 2, comparison of the distribution of the upwelling point intensity ($\theta=0$) from the cloud top is shown for $\tau=10$, where θ is the emergent angle with respect to the outward normal. The intensity distribution is shown along the corner line ($x/a=0$) and the center line ($x/a=0.5$). Note that intensity distributions along $y/a=0$ and 0.5 are identical to those along

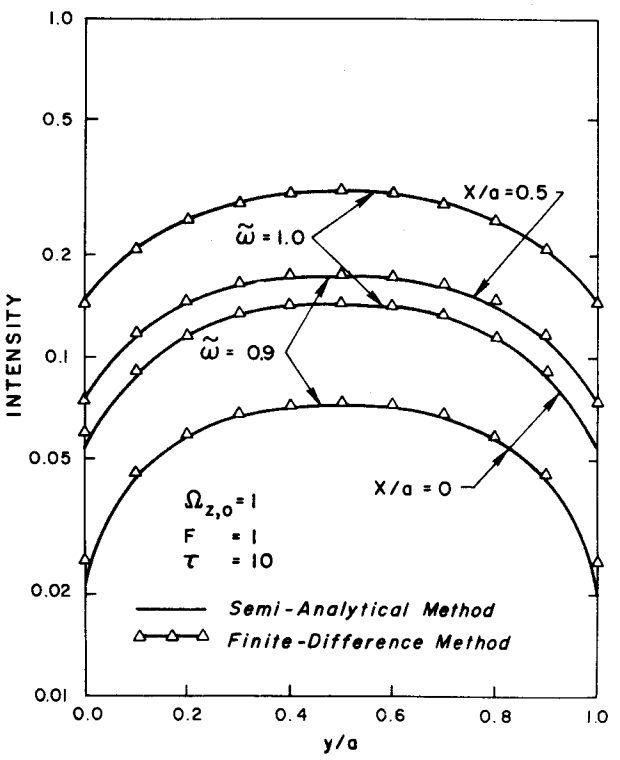

FIG. 2. Upward intensity distribution at the top of the cubic cloud with an optical depth of 10 along $x/a=0$ and 0.5 when the sun is overhead for two single-scattering albedos, 0.9 and 1.

$x/a=0$ and 0.5 owing to the geometrical symmetry when the sun is overhead. The absolute intensity differences between semianalytical and numerical methods are within about 0.006, or about 0.2% of the incident flux.

Figure 3 shows a comparable comparison for the upwelling point flux distribution at the cloud top for $\tau=10$, where the absolute differences are found to be less than 0.01, i.e., 0.3% of the incident flux. In general for τ in the range from 0.5 to 50, we find that the point-intensity and flux-density distributions computed from the numerical approach have similar accuracies to those cited above.

Figures 4–6 show the comparisons of single-face average intensity at selected angles and average flux density, respectively, as functions of the unilateral optical depth for a single-scattering albedo of 1. Shown in Fig. 4(a)–(e) are the average intensity for the top ($z=0$), the bottom ($z=a$), and one of the four side surfaces (e.g., $x=0$). The average intensity emergent from the side surface depends on the emergent angle and the azimuthal angle ϕ between the local zenith and the projection of the intensity on the side surface. In Fig. 4(c)–(e), average intensities are illustrated for three azimuthal planes, namely $\phi=0°$ (upward), 90° (or 270°) (horizontal), and 180° (downward), and for emergent angles θ of 0°, 30°, 60°, and 90°. We

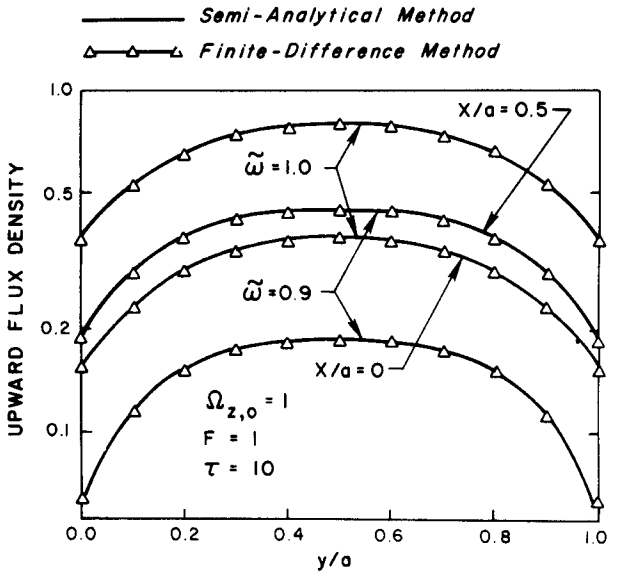

FIG. 3. Upward flux-density distribution at the top of a cubic cloud with an optical depth of 10 along $x/a=0$ and 0.5 when the sun is overhead for single-scattering albedos of 0.9 and 1.

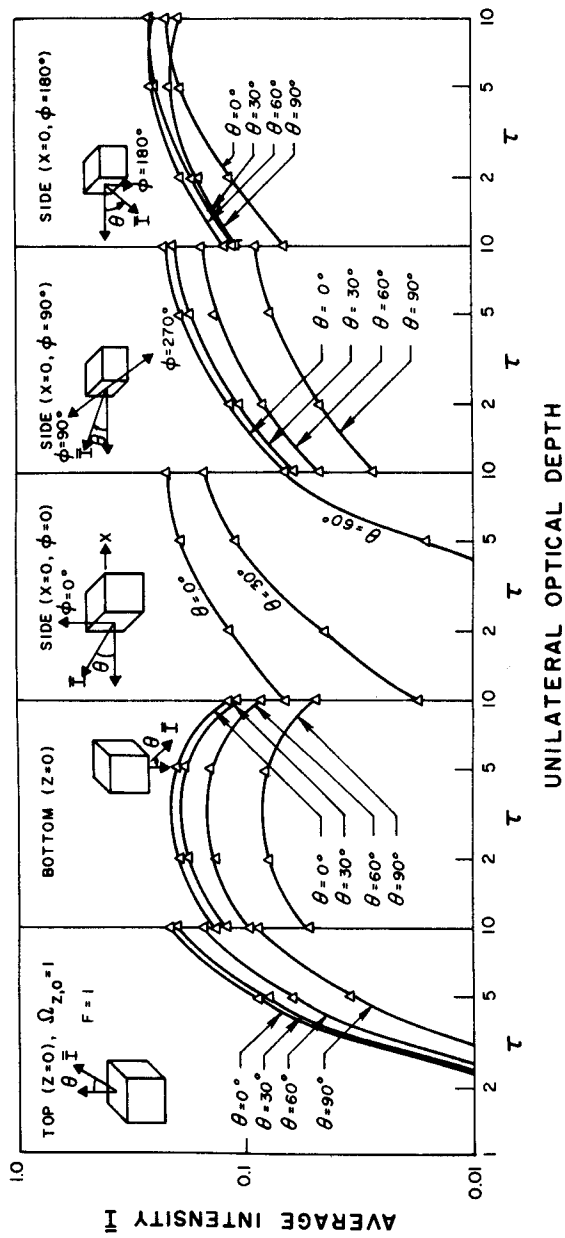

FIG. 4. Single-face average intensity emergent from the cloud faces as a function of unilateral optical depth for zenith angle of 0°, 30°, 60°, and 90° when the sun is overhead for conservative scattering: (a) top, (b) bottom, (c) side (upward), (d) side (horizontal), (e) side (downward).

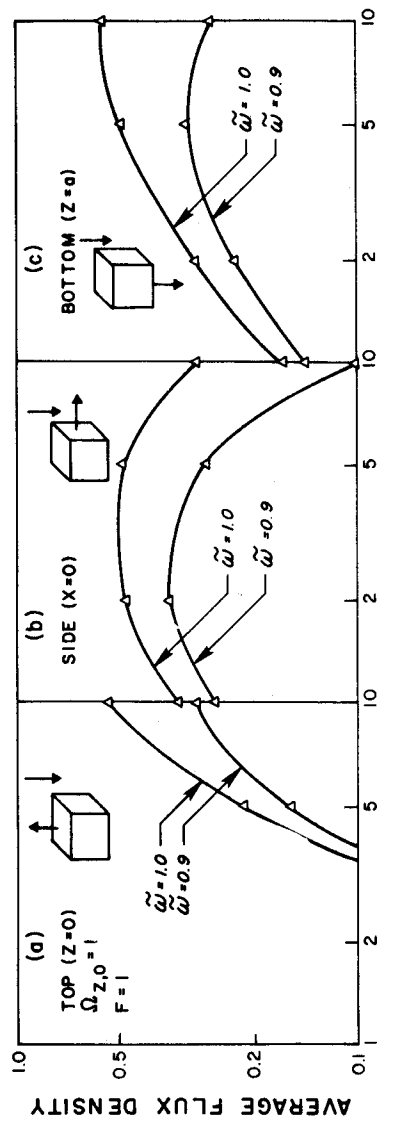

FIG. 5. Average outward flux density as a function of unilateral optical depth (a) at the cloud top, (b) at the cloud side, and (c) at the cloud bottom, for overhead sun and for single-scattering albedos of 0.9 and 1.

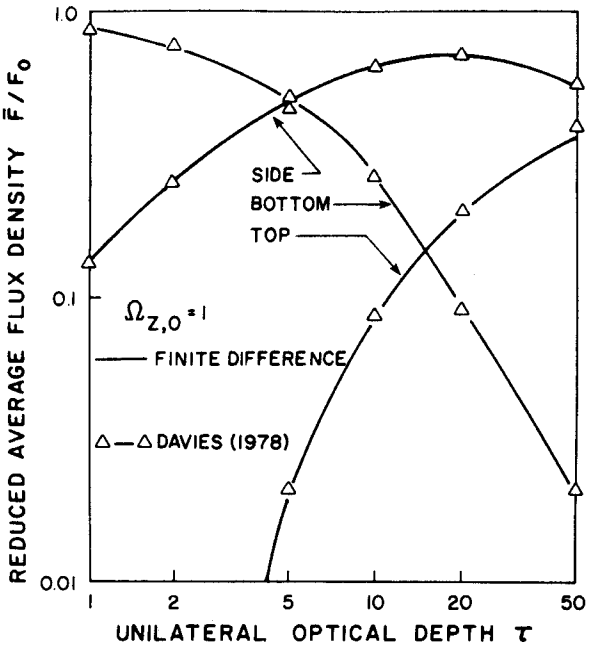

FIG. 6. Comparison of the average outward flux density as a function of the unilateral optical depth with results from the semianalytical method presented by Davies [3] for $\tilde{\omega}=1$ and overhead sun.

find again that the comparison between the two methods is satisfactory, for the resulting differences are less than about 0.01. It is interesting to note that upon increasing the optical depth the outward intensities increase on all faces except the bottom, on which the outward (transmitted) intensity first increases and then decreases. On the side surface, the average intensity as a function of θ and ϕ is found to be symmetric with respect to the line $\phi=0°$ (or 180°) due to the spherical-harmonic expansion employed in the analyses. This leads to $\bar{I}(\theta,\phi)=\bar{I}(\theta,-\phi)$.

Figure 5(a)–(c) shows the comparisons of the average outward diffuse flux density at the top, side, and bottom, respectively, for $\tilde{\omega}=1.0$ and 0.9. The differences between the two methods are all less than about 0.01. Moreover, these graphs show that absorption reduces the outward flux density. The upward flux density from the top surface increases as the optical depth increases. This increase is in accord with our understanding that the reflected flux density increases with increasing optical depth. In addition, for the downward flux density at the bottom, we also find the general increase as the optical depth increases. The increasing transmitted flux density is

compensated to a certain degree by the decreasing outward flux density from the four side walls for optical depths greater than about 2 to 3. Finally, we also compare the values of the average flux density calculated from the finite-difference method with the results presented by Davies [3], who utilized a similar semianalytical method in the transfer analyses. This is shown in Fig. 6. Note that in this comparison the direct component at the bottom has been included. Agreement within about 1% is found.

b. Oblique Solar Incidence

The case of arbitrarily oblique solar incidence on a cubic cloud has not been investigated rigorously and completely in the theoretical-analytical approach, owing to the complexity encountered in the evaluation of the direct-solar-radiation attenuation path length. A special case of the face-parallel oblique incidence has been studied by Davies [3], who used the method of equivalent normal flux approximation to reduce the original three-dimensional transfer equation to an equivalent one-dimensional form. The most comprehensive computations regarding the transfer of solar radiation in cubic clouds have been carried out by McKee and Cox [5] utilizing the Monte Carlo method, which requires extensive computer time in order to achieve adequate accuracy. The equivalent-normal-flux method was based on the assumption that the solution can be decomposed into two components, each of which can be obtained from a model cube with equivalent average transmitted solar flux on any cross section. It involves a certain degree of complexity. It is the purpose of the present numerical approach to solve the transfer equation in a more direct and realistic way and to reduce the computational effort to a minimum.

Following the algorithm outlined in Sec. 4, we proceed to compute the average intensity and flux density for the case of face-parallel solar incidence. Figure 7 shows the comparison of the area-weighted average intensity [see Eq. (24)] from the present numerical method with the results of Monte Carlo method presented by McKee and Cox [5] for $\tau = 9.8$. The asymmetry factor used in the calculations is 0.855, and the zenith angle used in this comparison is 60°. The abscissa is composed of two parts. The left-hand side is the emergent angle with respect to the normal at the shaded side for $\phi = 0°$, while the right-hand side is the emergent angle at the sunlit side for $\phi = 180°$. General agreement is found except in the region near 90° on the shaded side, where a prominent peak appears in the Monte Carlo result. It is believed that this difference is due to the first-order approximation in the spherical-harmonic expansion employed in the present analyses.

Additional comparisons have also been carried out between the present calculations and the graphs shown by McKee and Cox [5] for the average intensity at the cloud top, the sunlit side, and the shaded side for zenith

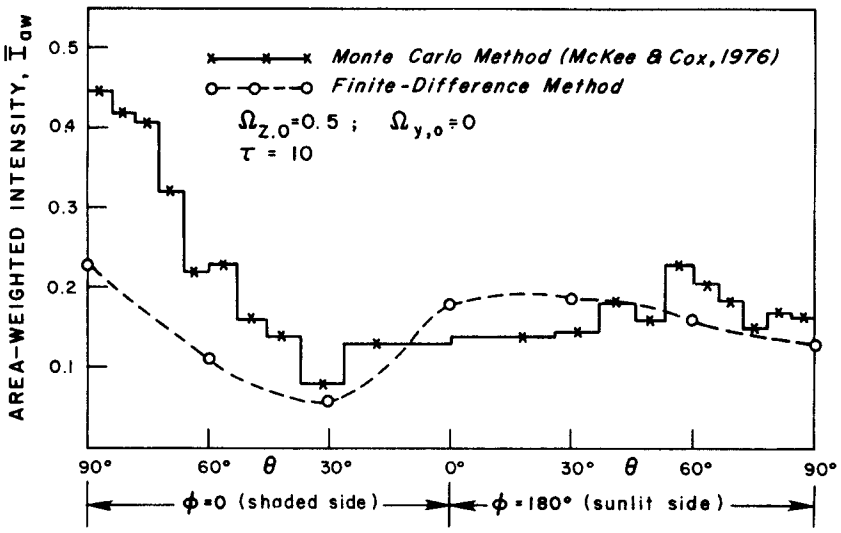

FIG. 7. Comparison of the area-weighted upward intensity from the finite-difference method with results from the Monte Carlo method presented by McKee and Cox [5] for $\tau = 9.8$, $\Omega_{x,0} = 0.5$, and $\Omega_{y,0} = 0$.

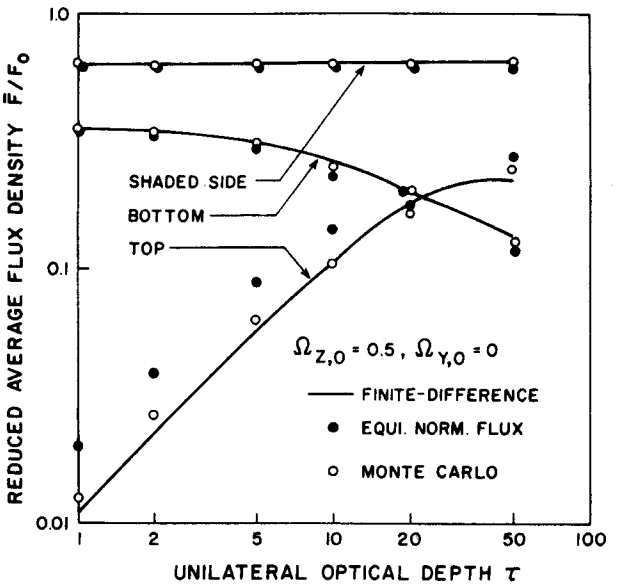

FIG. 8. Comparison of the average outward flux density at the top, the bottom, and the shaded side as a function of the unilateral optical depths with results from the Monte Carlo method and the equivalent-normal-flux method presented by Davies [3] for $\tilde{\omega} = 1$, $\Omega_{x,0} = 0.5$, and $\Omega_{y,0} = 0$.

angles of 30° and 60°. For optical depths of 9.8 and 73.5, comparisons of the present calculations with results from the Monte Carlo method are not as close as for the area-weighted intensity, especially in the regions where the peak intensities occur.

Figure 8 shows the comparison of the average flux density over the top, the bottom, and the shaded side with the results of both the Monte Carlo and the equivalent-normal-flux methods presented by Davies [3]. The direct component of the transmitted solar radiation is included in the flux-density values for the bottom and shaded side. It is evident that agreement of the present calculations with both sets of data is reasonably good. In all cases, however, the results from the present numerical approach show somewhat better agreement with those from the Monte Carlo method, because the optical path length is evaluated exactly according to the original geometry of the model without any modification.

7. CONCLUDING REMARKS

A numerical scheme using the finite-difference method to solve the three-dimensional partial differential equation derived from the solar transfer equation has been developed. Investigations and calculations have been performed for cases involving overhead solar incidence and face-parallel oblique solar incidence. For the overhead incidence case, results are compared with those from the semianalytical method in terms of the local and average intensity and flux density, and the comparisons reveal excellent agreement. For the oblique incidence case, computational results for the area-weighted intensity and average flux density are compared with those presented by previous investigators using the Monte Carlo method and the equivalent-normal-flux method. Good agreement again is obtained. These comparisons reveal that the present numerical approach could be a useful tool in tackling the three-dimensional solar-transfer problem. The method is most efficient for cases when the horizontal extent and vertical thickness of the cloud are of the same order. It can be applied to the case of arbitrarily oblique incidence of the solar beam. Finally, the numerical method can easily be modified for a group of cubic clouds horizontally distributed in the atmosphere to evaluate its reflection, absorption, and transmission properties.

Research supported in part by the Atmospheric Research Section of the National Science Foundation under Grants ATM75-05216 and ATM78-26259.

REFERENCES

1 K. M. Case and P. F. Zweifel, *Linear Transport Theory*, Addison-Wesley, Reading, Mass., 1967, 342 pp.
2 S. Chandrasekhar, *Radiative Transfer*, Dover, New York, 1960, 393 pp.
3 R. Davies, The effect of finite geometry on the three dimensional transfer of solar irradiance in clouds, *J. Atmospheric Sci.* 35:1712–1725 (1978).
4 K. N. Liou and S. C. Ou, Infrared radiative transfer in finite cloud layers, *J. Atmospheric Sci.* 36: 1985–1996 (1979).
5 T. B. McKee and S. K. Cox, Simulated radiance patterns for finite cubic clouds, *J. Atmospheric Sci.* 33:2014–2020 (1976).
6 D. L. Powers, *Boundary Value Problems*, Academic, New York, 1972, 238 pp.